

Supporting Information

Tailoring Zero-Point Energies in Nanocrystalline 3D Hofmann-Type Spin-Crossover Networks $\{\text{Fe}_{1-x}\text{M}_x(\text{pz})[\text{Pd}(\text{CN})_4]\}$: Impact of Size, Composition, and Surrounding Matrices

Chinmoy Das¹, Ajana Dutta², Denisa Coltuneac³, Laurentiu Stoleriu³, Pradip Chakraborty^{1*}

¹Department of Chemistry, Indian Institute of Technology Kharagpur, Kharagpur-721302, India

²Department of Physics, Indian Institute of Technology Kharagpur, Kharagpur-721302, India

³Faculty of Physics, Al. I. Cuza University, 700506 Iasi, Romania

*Corresponding Author, E-mail: pradipc@chem.iitkgp.ac.in

HRTEM images:

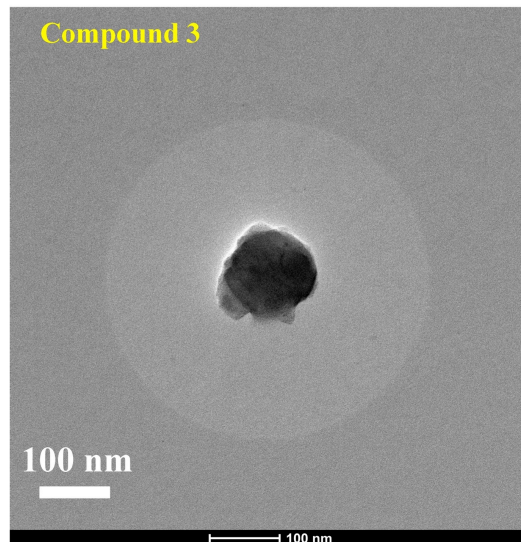
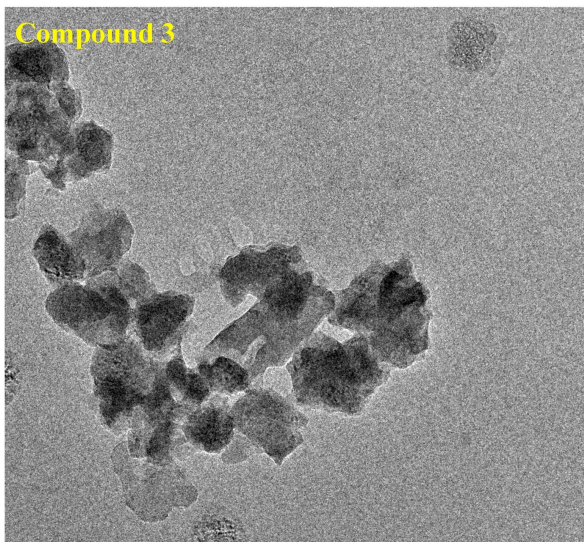
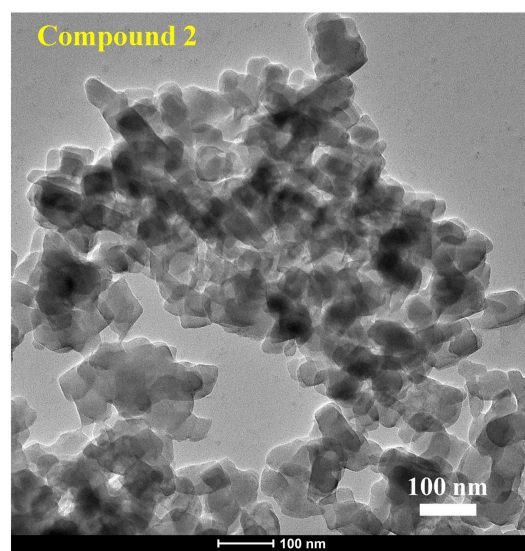
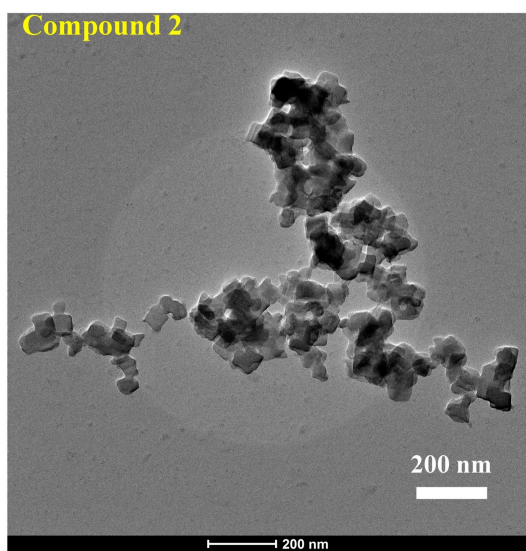
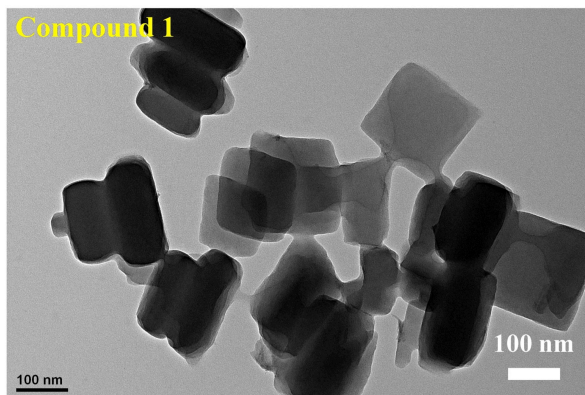
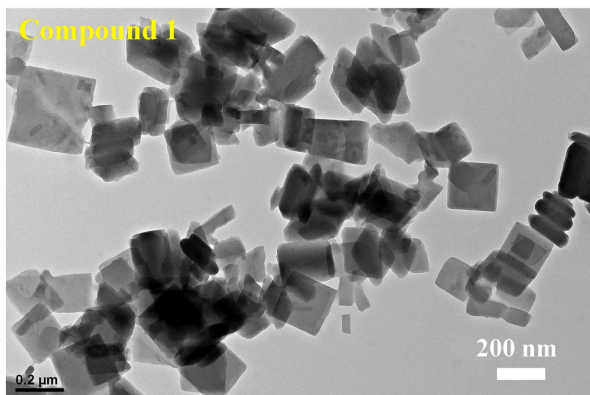


Figure S1: High-resolution TEM images of as-synthesized nanocrystals (compound 1, compound 2 and compound 3)

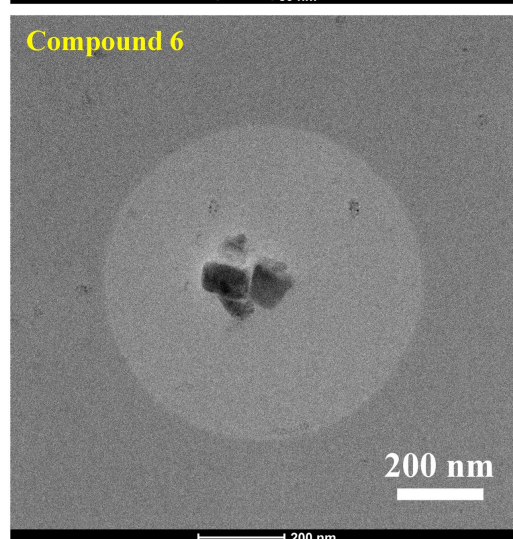
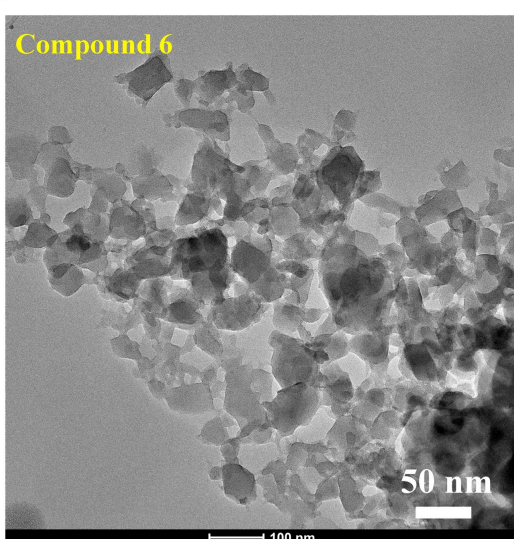
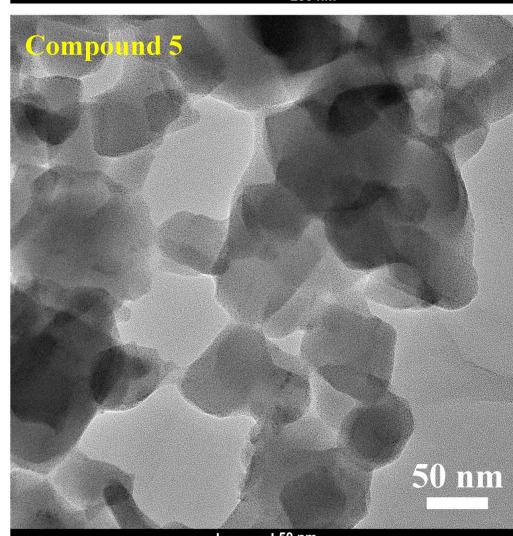
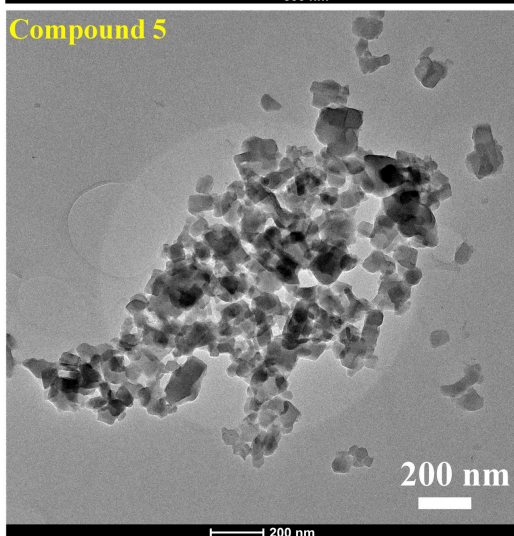
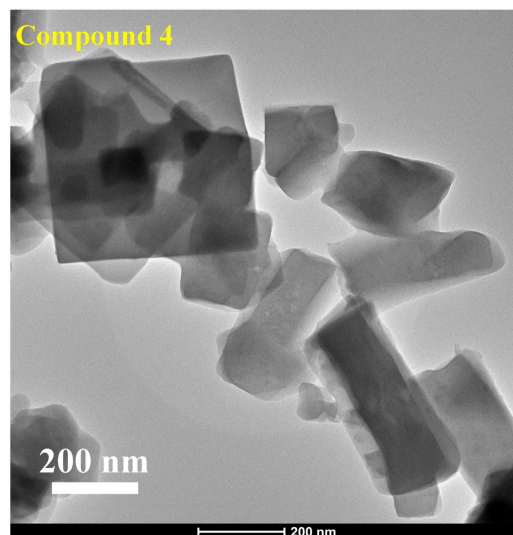
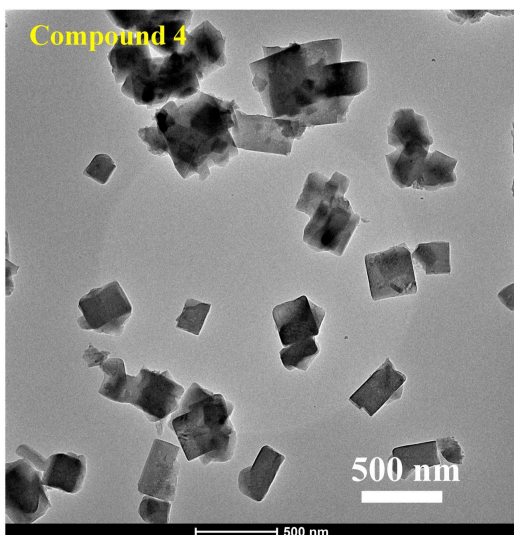


Figure S2: High-resolution TEM images of as-synthesized nanocrystals (compound 4, compound 5 and compound 6)

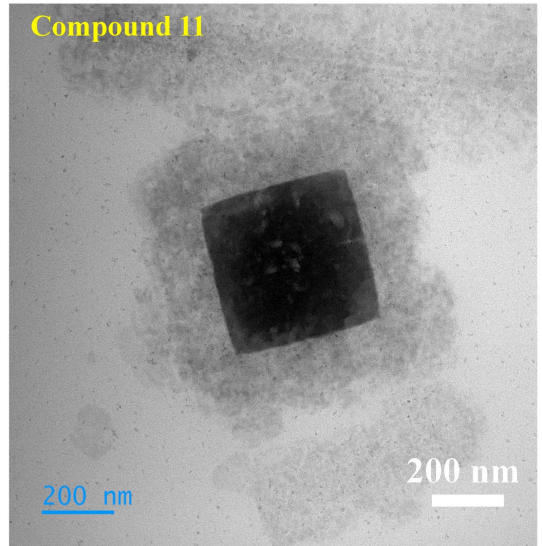
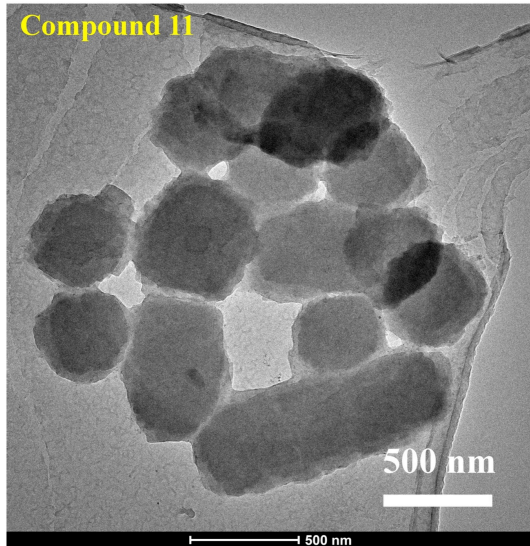
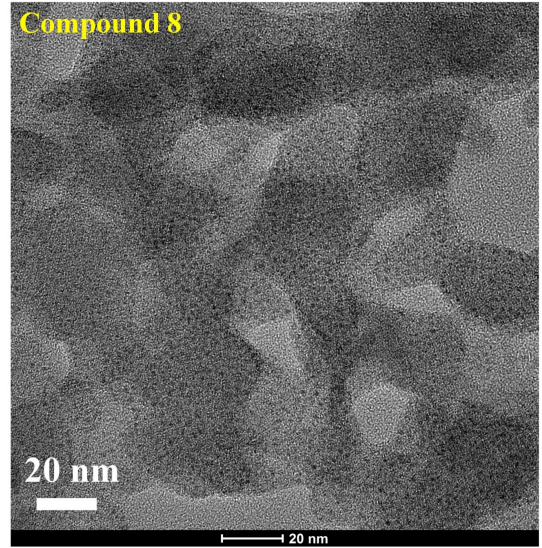
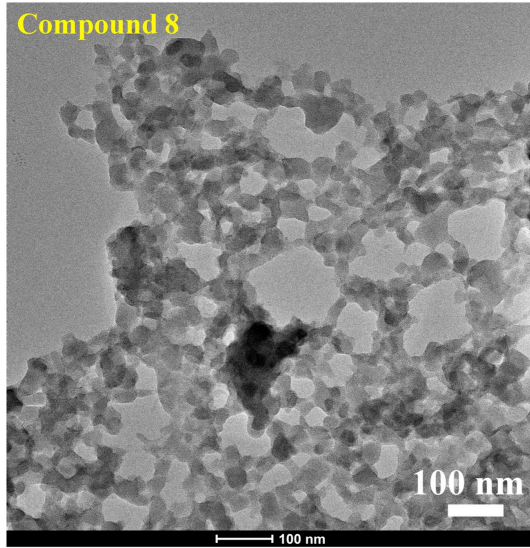
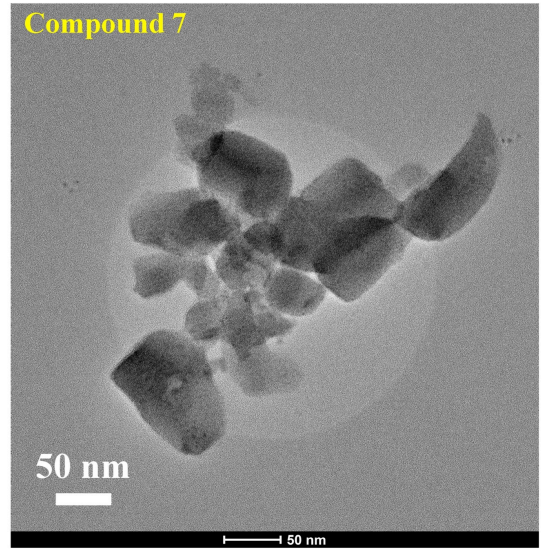
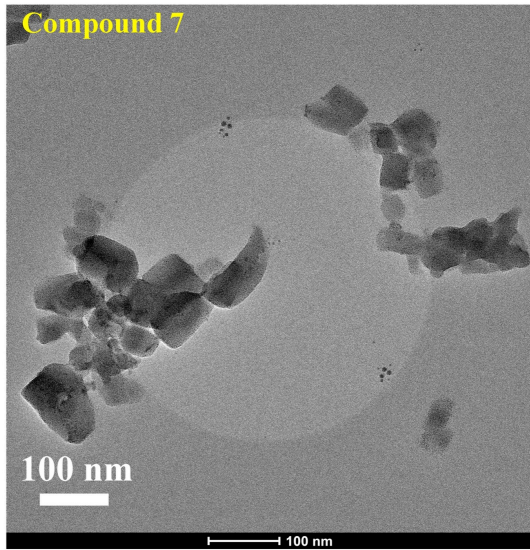


Figure S3: High-resolution TEM images of as-synthesized nano- and submicrocrystals (compound 7, compound 8 and compound 11)

EDX Spectrum:

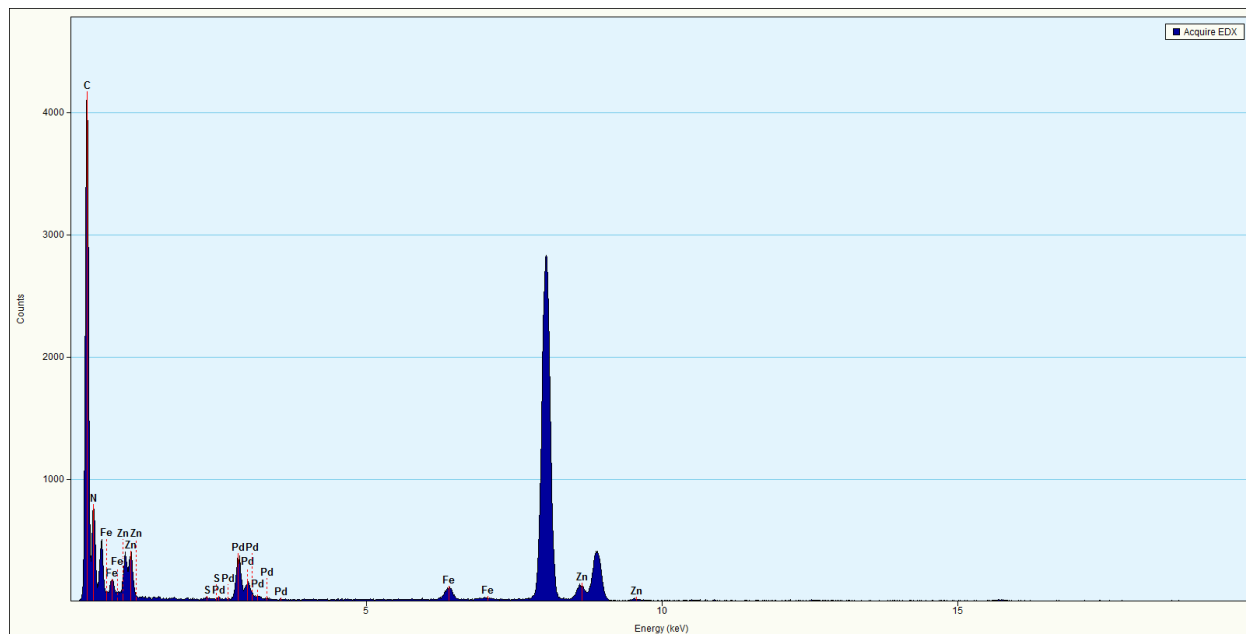


Figure S4. EDX spectrum of compound 3; effective composition $[\text{Fe}_{0.37}\text{Zn}_{0.63}(\text{pz})\text{Pd}(\text{CN})_4]$

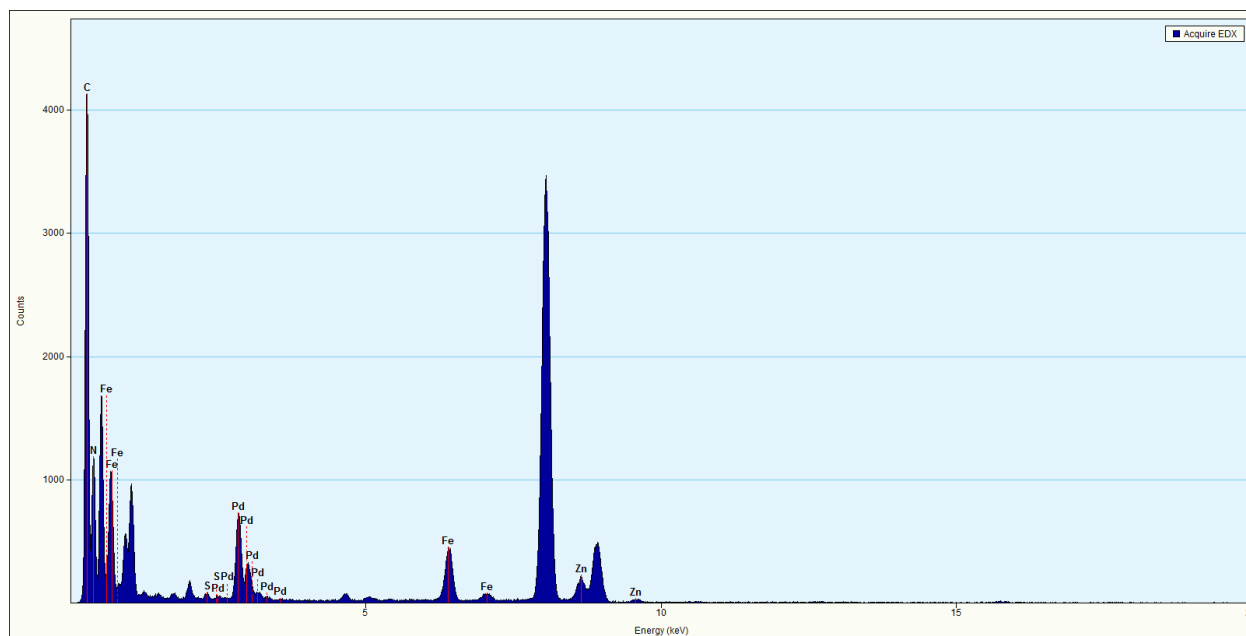


Figure S5. EDX spectrum of compound 4; effective composition $[\text{Fe}_{0.66}\text{Zn}_{0.34}(\text{pz})\text{Pd}(\text{CN})_4]$

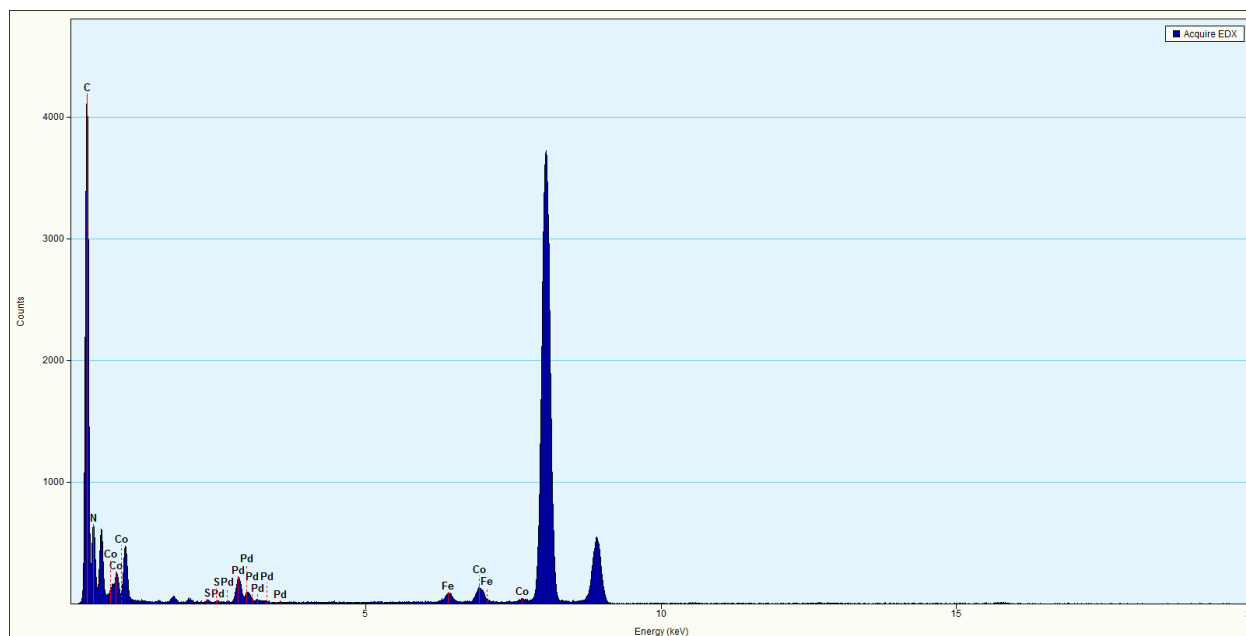


Figure S6. EDX spectrum of compound 5; effective composition $[\text{Fe}_{0.32}\text{Co}_{0.68}(\text{pz})\text{Pd}(\text{CN})_4]$

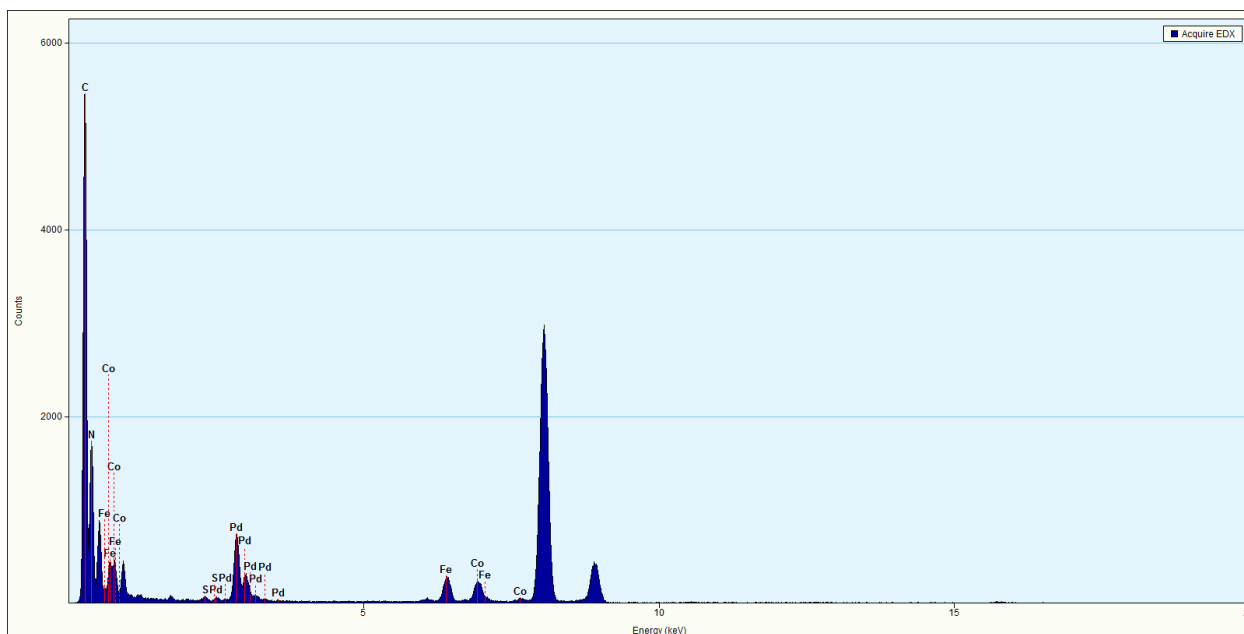


Figure S7. EDX spectrum of compound 6; effective composition $[\text{Fe}_{0.54}\text{Co}_{0.46}(\text{pz})\text{Pd}(\text{CN})_4]$

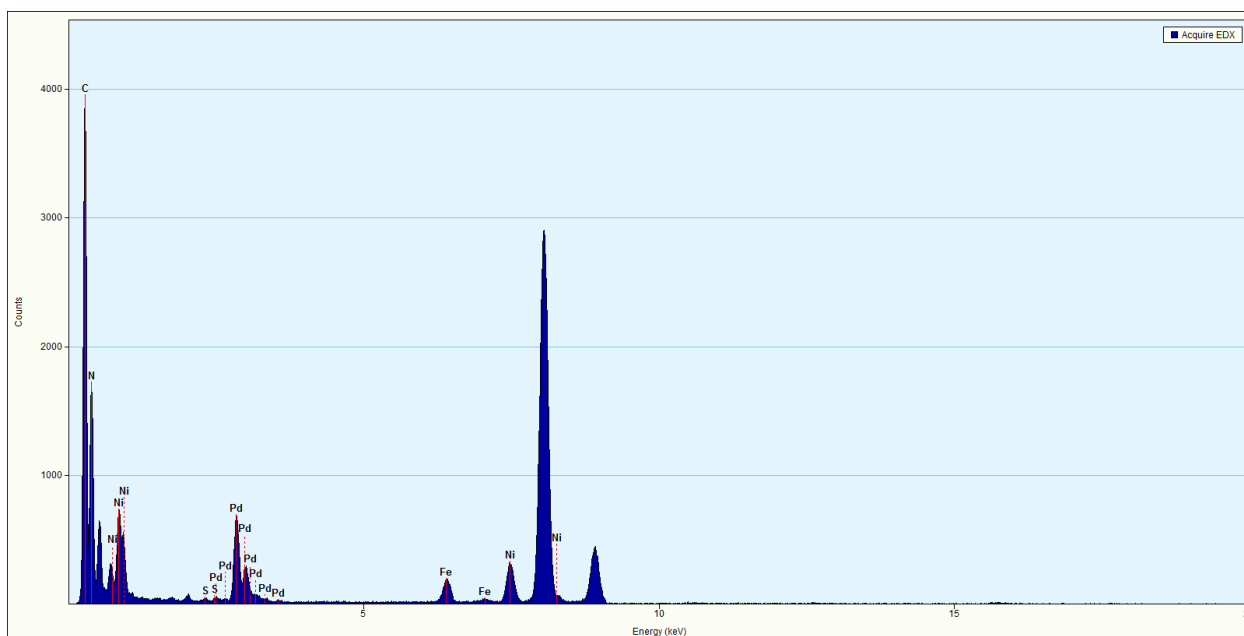


Figure S8. EDX spectrum of compound 7; effective composition $[\text{Fe}_{0.36}\text{Ni}_{0.64}(\text{pz})\text{Pd}(\text{CN})_4]$

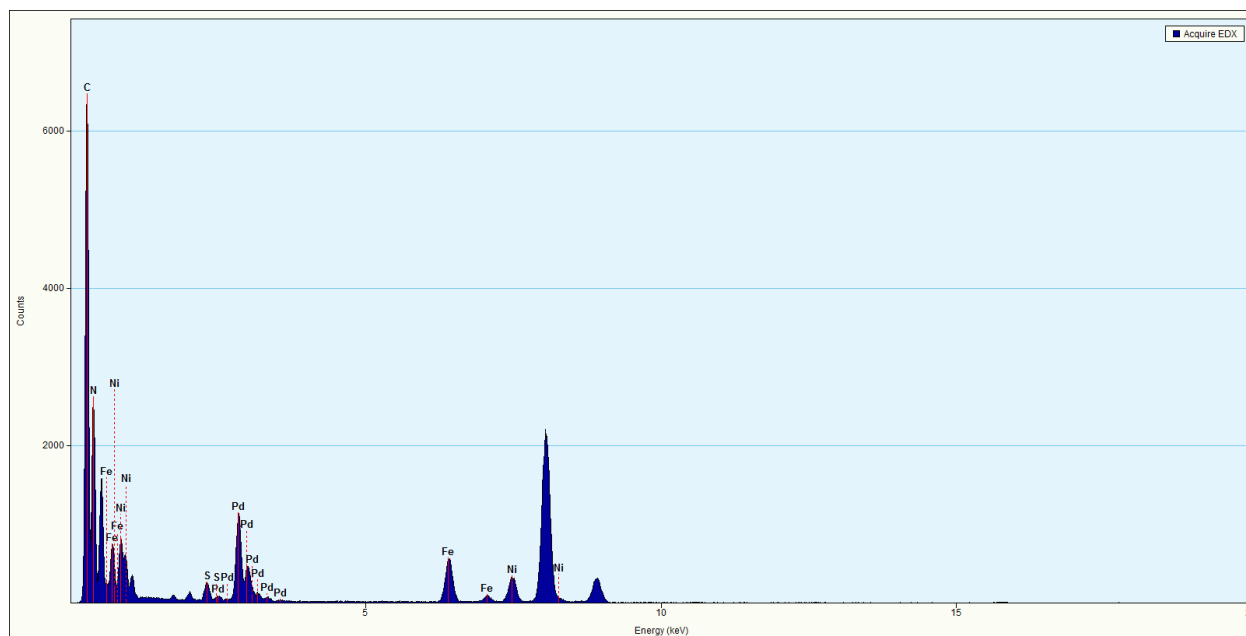


Figure S9. EDX spectrum of compound 8; effective composition $[\text{Fe}_{0.62}\text{Ni}_{0.38}(\text{pz})\text{Pd}(\text{CN})_4]$

FTIR Spectrum:

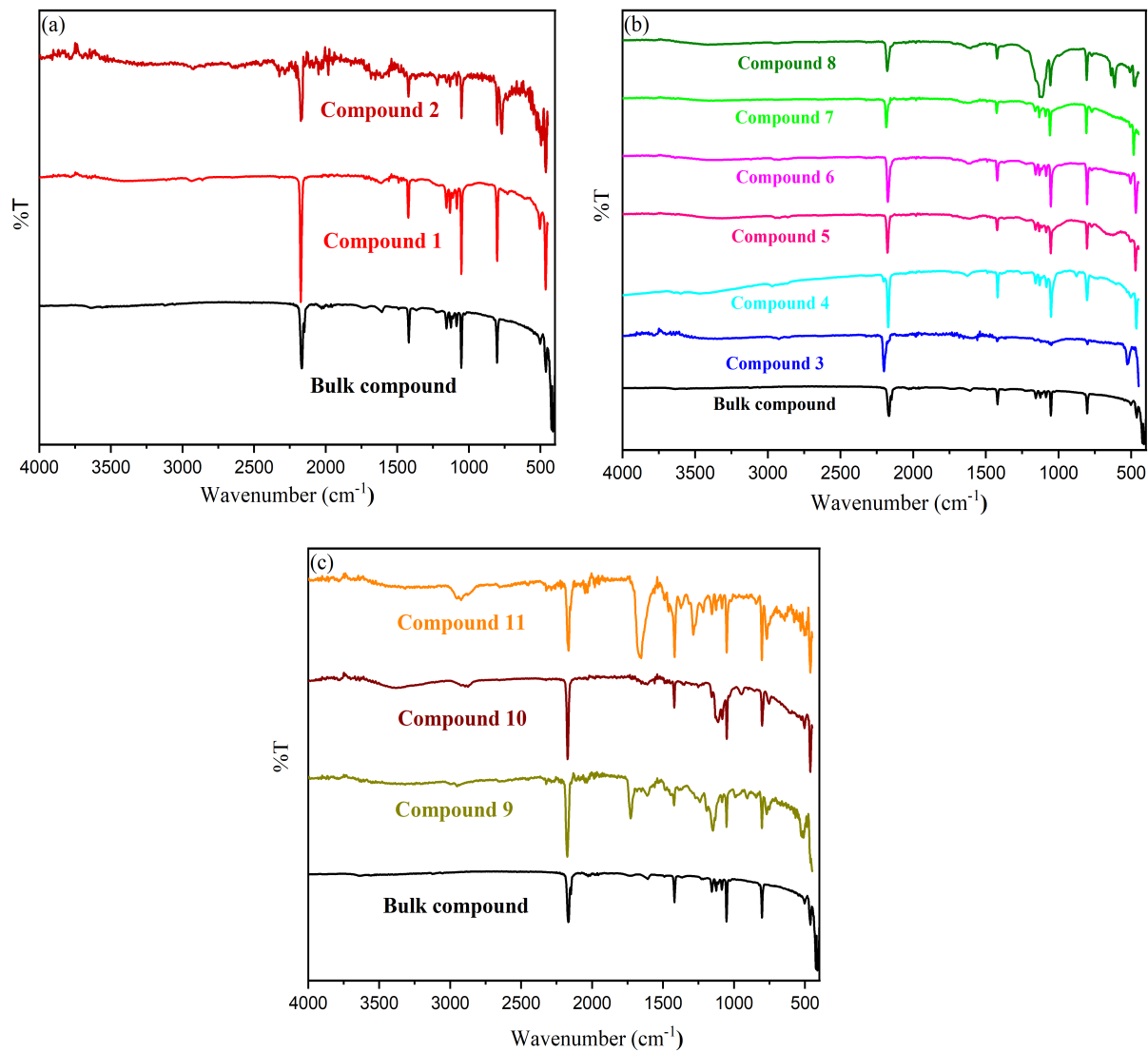
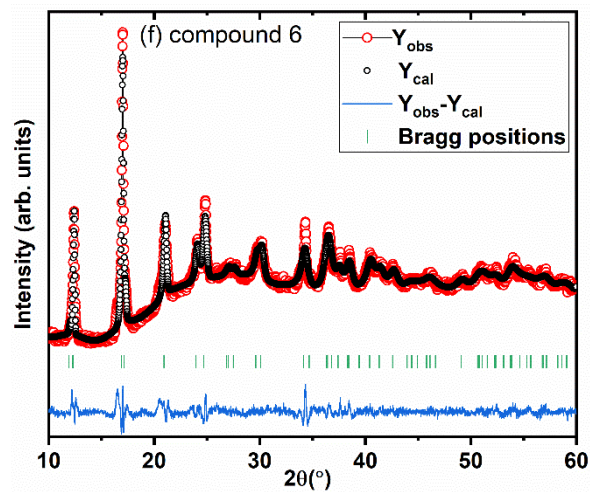
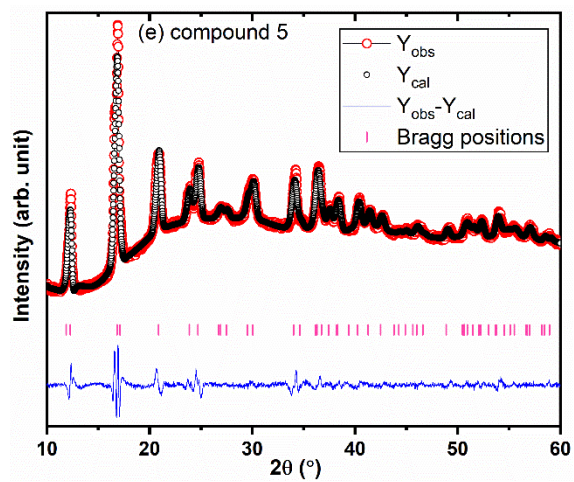
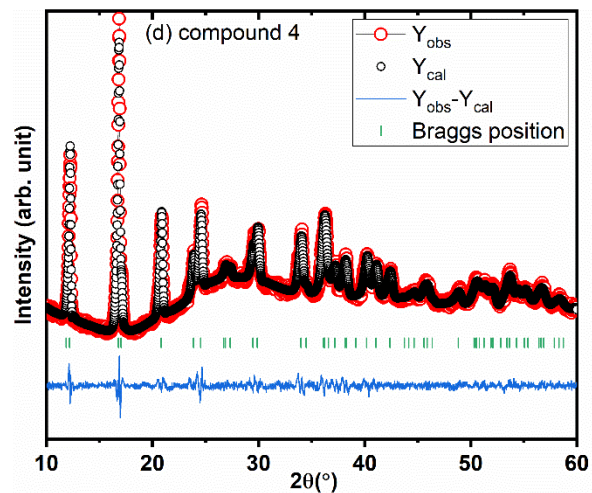
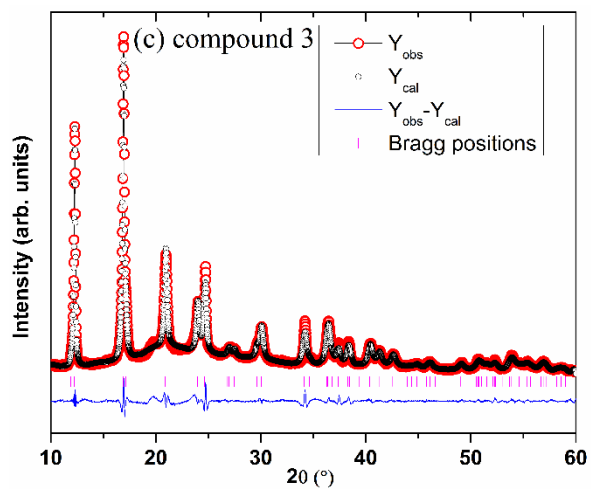
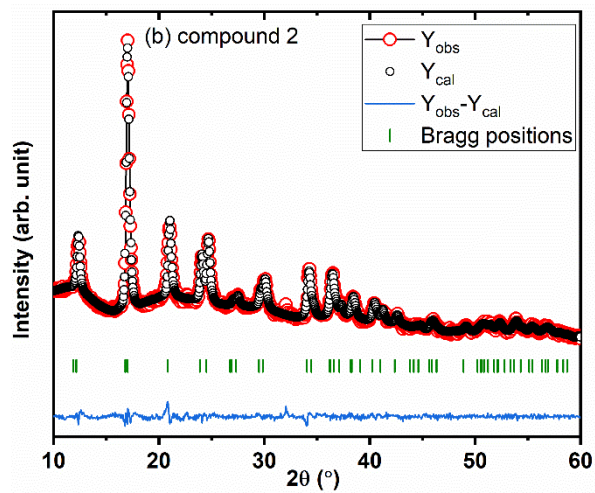
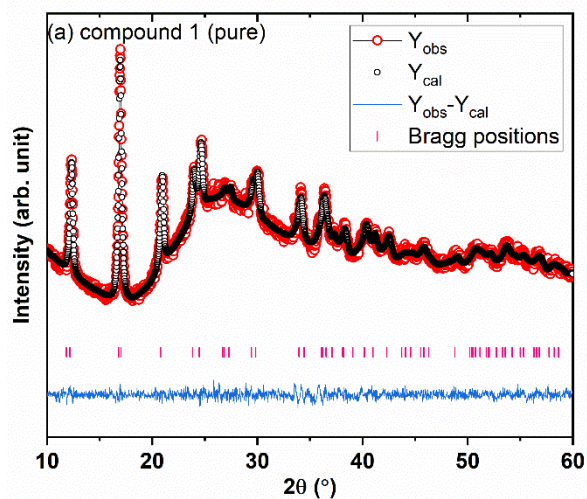


Figure S10. FTIR spectra of the desired as-synthesized Hofmann-based nanoparticles along with the bulk compound with generic formula $[\text{Fe}_{1-x}\text{M}_x(\text{pz})\text{Pd}(\text{CN})_4]$; (a) Compounds 1-2; (b) Compounds 3-8; (c) Compounds 9-11

Table S1. Selected major peaks from the FTIR spectra of the as-synthesized nanoparticles.

Bond Type	Wavenumber (cm⁻¹)	Peak intensity
Fe-N (pz)	411	Broad
Fe-N (CN ⁻)	411	Broad
Pd-C (CN ⁻)	802	Strong
C=N (pz)	1419	Medium
C=C (pz)	1053	Strong
C≡C (CN ⁻)	2166 (Characteristic peak)	Strong

Refined PXRD pattern:



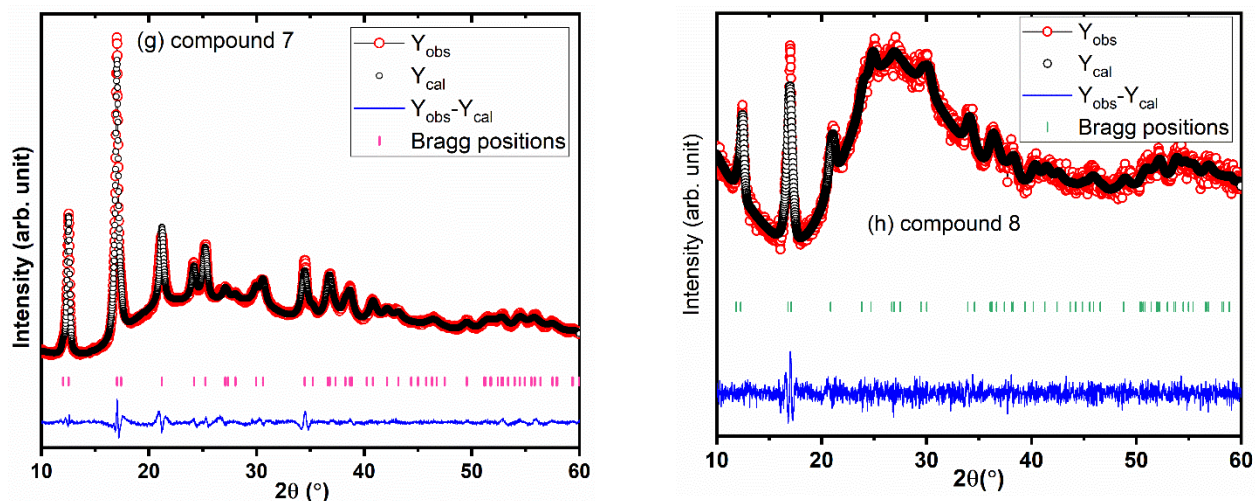


Figure S11. PXRD Le Bail profile refinement of (a) pure $[\text{Fe}(\text{pz})\text{Pd}(\text{CN})_4]$ (~ 157 nm) (compound 1), (b) pure $[\text{Fe}(\text{pz})\text{Pd}(\text{CN})_4]$ (~ 55 nm) (compound 2), (c) 63% Zn (compound 3), (d) 34% Zn (compound 4), (e) 68% Co (compound 5), (f) 46% Co (compound 6), (g) 64% Ni (compound 7) and (h) 38% Ni (compound 8) at room temperature.

Table S2. Variation in FWHM for (110) peak in compounds 1-8 compared to the bulk analog

Compounds Name	FWHM for (110) peak (in degree)
Bulk $[\text{Fe}(\text{pz})\text{Pd}(\text{CN})_4]$	0.08764 (± 0.00338)
Compound 1	0.2832 (± 0.00523)
Compound 2	0.29949 (± 0.01595)
Compound 3	0.21996 (± 0.00517)
Compound 4	0.18322 (± 0.0168)
Compound 5	0.25468 (± 0.01077)
Compound 6	0.18043 (± 0.00409)
Compound 7	0.29131 (± 0.00713)
Compound 8	0.31024 (± 0.0075)